

# Defining Hydrophobicity: Probing the Structure of Solute-Induced Hydration Shells by Fourier Transform Infrared Spectroscopy

David Hecht, Lema Tadesse, and Lee Walters\*

Contribution from The Scripps Research Institute, Department of Molecular Biology, MB-15, La Jolla, California 92037. Received October 28, 1991

**Abstract:** Systematic differences exist in the vibrational transitions of water molecules that are associated with the hydration of solutes containing varying numbers of methylene or methyl groups. Model solutions studied contained individual members of a series of alkanesulfonates. Observed shifts in the vibrational intensities and frequencies of solvating water molecules are consistent with an increase in the number of solvent-solvent intermolecular hydrogen bonds as the hydrocarbon moiety of the alkanesulfonate increases in size. These data are consistent with theories of aqueous solvation in which hydration shells become progressively more structured and thermodynamically stable as the "hydrophobicity" of the dissolved solute increases.

## Introduction

Hydrophobic effects play a critical role in many chemical reactions and in the organization of biologically important molecules and cellular structures. Prominent examples include the rates of aldol additions,<sup>1</sup> solvent-dependent chemoselectivity,<sup>2</sup> the folding pathways and tertiary structures of native proteins, the clustering of aromatic nitrogenous bases in DNA and RNA molecules, and the stability of biological membranes in aqueous environments. Hydrophobic effects are important in molecular recognition processes as diverse as antibody-antigen, enzyme-substrate, receptor-hormone, cyclodextrin<sup>3</sup> and crown ether-ligand binding,<sup>4</sup> and the interactions of chemotherapeutic drugs with DNA.<sup>5</sup> In this report we demonstrate a strategy, based upon Fourier transform infrared spectroscopy (FTIR), that provides fundamental insights into the structural perturbations of bulk water that are caused by hydrophobic solutes and that provides a structure-oriented conceptual framework for evaluating a wide range of hydrophobic effects.

It has been proposed that the unfavorable free energies associated with the dissolution of hydrocarbons in water at  $\sim 20^\circ\text{C}$  are caused by a net decrease in entropy due to increased numbers of hydrogen bonds in solute-induced hydration shells.<sup>6</sup> Increased ordering of solvation shells has been inferred from calorimetric measurements of  $\Delta C_{p,2}^\circ$ ,<sup>7</sup> the excess molar heat capacity.<sup>8</sup>  $\Delta C_{p,2}^\circ$  has been considered an indicator of the extra energy that is needed to "melt" the presumably ordered water that surrounds dissolved hydrocarbons and, therefore, has been used as a measurement of hydrophobicity.<sup>8</sup> In addition to calorimetry, measurements of hydrophobicity have been based upon the relative solubilities of solutes in aqueous and nonaqueous phases.<sup>6,9</sup> The resulting

hydrophobicity scales are dependent upon the solvents and phases that are used. In the special case of amino acids, hydrophobicities have been assigned according to the relative accessibilities of side chains to solvent in native, folded proteins.<sup>10</sup>

The formulation of a comprehensive theory of hydrophobicity and hydrophobic effects will require detailed structural information about solute-solvent and solvent-solvent interactions.<sup>8,9,11</sup> An important source of this information can be the vibrational transitions originating in solute-induced hydration shells. Infrared spectroscopy has been used previously to detect the vibrations of DOH molecules in the solvation shells of inorganic salts.<sup>12</sup> The data presented below demonstrate systematic differences in the spectra of water molecules associated with the solvation shells of solutes that contain varying numbers of methylene or methyl groups.

## Experimental Section

**Sample Preparation.** Aqueous solutions (100 mM) of sodium methane-, ethane-, propane-, butane-, pentane-, and hexanesulfonate were prepared from  $\geq 98\%$  pure compounds (Aldrich). The purity of each alkanesulfonate was confirmed by two methods. First, each compound gave a single spot by thin layer chromatography (Whatman K6 silica gel plates; mobile phase, ethyl acetate/acetic acid/water, 3:1:1, v/v/v; spot detection, 10% aqueous silver nitrate and 0.2 g of sodium fluorescein in 100 mL of absolute ethanol, 1:5, v/v).<sup>13</sup> TLC was performed on each sample solution in duplicate. Second, each compound appeared homogeneous without detectable impurities when examined, as a 100 mM aqueous solution, by FTIR (purity of the compounds was judged by comparison with the data presented in the *Aldrich Library of Infrared*

(1) Heathcock, C. H. Stereoselective Aldol Condensations. In *Comprehensive Carbanion Chemistry Part B*; Buncl, E., Durst, T., Eds.; Elsevier: Amsterdam, 1984; p 177 ff.

(2) (a) Krishnamurthy, S.; Brown, H. *J. Org. Chem.* **1980**, *45*, 2550. (b) House, H. O.; Lee, T. V. *J. Org. Chem.* **1978**, *43*, 4369.

(3) Breslow, R. *Acc. Chem. Res.* **1991**, *24*, 159.

(4) (a) Cram, D.; Doxsee, K. *J. Org. Chem.* **1986**, *51*, 5068. (b) Doxsee, K.; Feigel, M.; Stewart, K. D.; Canary, J. W.; Knobler, C. B.; Cram, D. *J. Am. Chem. Soc.* **1987**, *109*, 3098. (c) Cram, D.; Carmack, R. A.; deGrandpre, M. P.; Lein, G. M.; Goldberg, I.; Knobler, C. B.; Maverick, E. F.; Trueblood, K. N. *J. Am. Chem. Soc.* **1987**, *109*, 7068.

(5) (a) Reich, E. *Cancer Res.* **1963**, *23*, 1438. (b) Dimarco, A.; et al. *Tumori* **1963**, *49*, 235. (c) Arcamone, F.; et al. *Biotechnol. Bioeng.* **1969**, *11*, 1101. (d) Ding, W.; Ellestad, G. A. *J. Am. Chem. Soc.* **1991**, *113*, 6617.

(6) (a) Kauzmann, W. *Adv. Protein Chem.* **1959**, *14*, 1. (b) Frank, H. S.; Evans, M. W. *J. Chem. Phys.* **1945**, *13*, 507.

(7)  $\Delta C_{p,2}^\circ$  is defined as being the difference between the partial molar heat capacity of a nonpolar solute at infinite dilution in aqueous solution and the molar heat capacity of the pure liquid solute.

(8) (a) Mirejovsky, D.; Arnett, E. M. *J. Am. Chem. Soc.* **1983**, *105*, 1112. (b) Gill, S. J.; Dec, S. F.; Olofsson, G.; Wadso, I. *J. Phys. Chem.* **1985**, *89*, 3758. (c) Muller, N. *Acc. Chem. Res.* **1990**, *23*, 23.

(9) (a) Nozaki, Y.; Tanford, C. *J. Biol. Chem.* **1971**, *246*, 2211. (b) Wolfenden, R.; Andersson, L.; Cullis, P. M.; Southgate, C. C. B. *Biochemistry* **1981**, *20*, 849. (c) Ben-Naim, A. *Hydrophobic Interactions*; Plenum Press: New York, 1980.

(10) (a) Chothia, C. *Nature* **1974**, *248*, 338. (b) Chothia, C. *J. Mol. Biol.* **1976**, *105*, 1. (c) Janin, J. *Nature* **1979**, *277*, 491. (d) Eisenberg, D.; Weiss, R. M.; Terwilliger, T. C.; Wilcox, W. *Faraday Symp. Chem. Soc.* **1982**, *17*, 109. (e) Kyte, J.; Doolittle, R. F. *J. Mol. Biol.* **1982**, *157*, 105. (f) Sweet, R.; Eisenberg, D. *J. Mol. Biol.* **1983**, *171*, 479. (g) Chothia, C. *Annu. Rev. Biochem.* **1984**, *53*, 537. (h) Rose, G. D.; Geselowitz, A. R.; Lesser, G. J.; Lee, R. H.; Zehfus, M. H. *Science* **1985**, *229*, 834.

(11) (a) Reynolds, J. A.; Gilbert, D. B.; Tanford, C. *Proc. Natl. Acad. Sci., U.S.A.* **1974**, *71*, 2925. (b) Sharp, K.; Nicholls, A.; Fine, R.; Honig, B. *Science* **1991**, *252*, 10. (c) Rossky, P. J.; Karplus, M. *J. Am. Chem. Soc.* **1979**, *101*, 1913. (d) Rossky, P. J.; Karplus, M.; Rahman, A. *Biopolymers* **1979**, *18*, 825.

(12) (a) Kristiansson, O.; Eriksson, A.; Lindgren, J. *Acta Chem. Scand., Ser. A* **1984**, *38*, 609. (b) Kristiansson, O.; Eriksson, A.; Lindgren, J. *Acta Chem. Scand., Ser. A* **1984**, *38*, 61. (c) Lindgren, J.; Kristiansson, O.; Paluszkiwicz, C. Infrared studies of Ionic Hydration in Aqueous Solutions. In *Interactions of Water in Ionic and Nontonic Hydrates*; Kleeberg, H., Ed.; Springer-Verlag: Berlin, 1987; p 43. (d) Kristiansson, O.; Lindgren, J.; Villepin, J. *J. Phys. Chem.* **1988**, *92*, 2680. (e) Bergström, P.-A.; Lindgren, J. *J. Mol. Struct.* **1990**, *239*, 103.

(13) (a) Pollard, F. H.; Nickless, G.; Burton, K. W. C. *J. Chromatogr.* **1962**, *8*, 507. (b) Coyne, C. M.; Maw, G. A. *J. Chromatogr.* **1964**, *14*, 552.

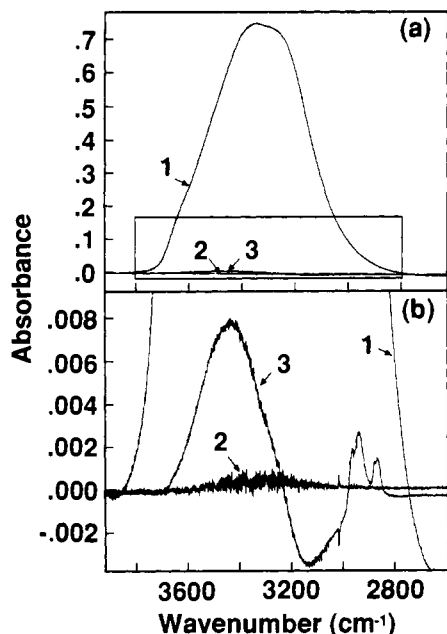


**Figure 1.** (a) Spectrum 1 is the absorption spectrum of pure water. Spectrum 2 shows the difference that results from subtracting two independently measured water samples, demonstrating the reproducibility of the measurement process and the relevant signal-to-noise ratio. Spectrum 3 is the difference spectrum of aqueous 100 mM sodium hexanesulfonate [(spectrum of hexanesulfonate solution) - (spectrum of pure water)]. (b) A portion of the boxed region in part a, with the scale of the ordinate expanded by a factor of 85.

Spectra and by the absence of any detectable, nonassignable absorbance peaks).

The water used to prepare all solutions and used in all measurements was deionized and filtered ( $\leq 5.6 \times 10^{-8}$  S-cm $^{-1}$ ; pore size = 0.22  $\mu$ m; Millipore).

**Infrared Techniques.** All spectra were measured on a Nicolet 740 FTIR spectrometer equipped with a HgCdTe detector; 3600 single-sided interferograms were averaged for each sample, with 8192 data points on the far side of the centerburst providing 2-cm $^{-1}$  resolution; 65 536 points were Fourier transformed, and no apodization was performed, i.e., a boxcar apodization function was used. Alternatively, for each spectrum, the 8192 data points were Fourier processed using a total of only 16 384 transform points and a triangular apodization function. No significant differences were found between any pair of spectra resulting from either 65 536 (boxcar apodization) or 16 384 (triangular apodization) transform points (data not shown). Samples were examined by attenuated internal reflectance, in duplicate experiments, in microcircle cells (path length  $\sim 7.5$   $\mu$ m, SpectraTech) containing ZnSe or GeAsSe crystals (45° conical ends), respectively. All samples were measured at pH 7.0  $\pm$  0.1 and 24.0  $\pm$  0.1 °C.

**Data Analysis.** The term "difference spectrum", as used in this report, is defined as follows: The difference spectrum associated with a sample solution = [(spectrum of a solution containing a particular solute) - (spectrum of pure water)]. Difference spectra were smoothed using a maximum likelihood algorithm<sup>14</sup> (ESmooth; Galactic Industries Corp.).

Each difference spectrum was corrected to account for the exclusion of water molecules from a given volume of the solution, compared to an identical volume of pure solvent, because of the physical space occupied by the relevant solute (the presence of solute caused small differences in the absolute amount of water in the optical beam path of the internal reflectance cell). Each correction factor was determined by measuring the liquid volume expansion that occurred when the relevant solute was dissolved in water to form a 100 mM sample solution. Each volume increase was measured by quantitatively dissolving an appropriate amount of solute (determined in preliminary measurements) in 100.00 mL of water in a specially modified and calibrated volumetric flask, maintained at a constant temperature of 24.0  $\pm$  0.1 °C, such that the final sample concentration was 100 mM. Final volume measurements were made 4 h after dissolution to ensure adequate temperature equilibration. It was determined that waiting 24–48 h did not result in any

(14) Freiden, B. R. *Deconvolution, With Applications in Spectroscopy*; Academic Press: New York, 1984; p 229.

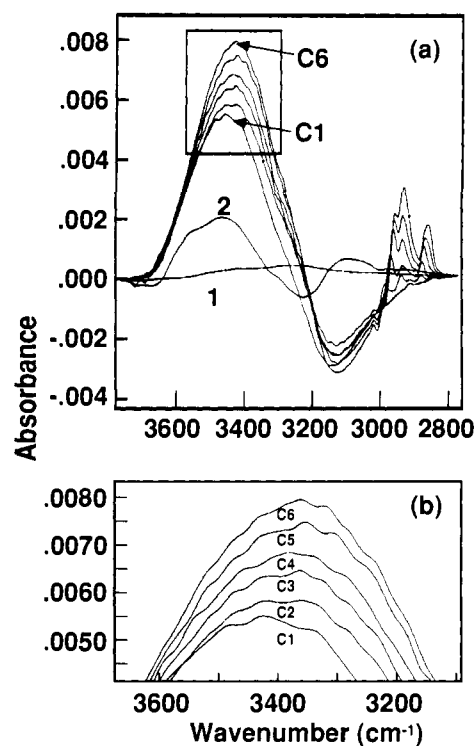


**Figure 2.** (a) Individual difference spectra of aqueous 100 mM alkane-sulfonate solutions. Each difference spectrum results from the average of two or more independently measured sample spectra, with spectra exhibiting a variation of less than  $4 \times 10^{-4}$  absorbance units prior to averaging. Spectrum 1 is the difference that results from subtracting two independently measured water samples. Spectrum 2 is the difference spectrum of 100 mM Na<sub>2</sub>SO<sub>4</sub> and pure water. The difference spectra C1–C6 represent 100 mM solutions of sodium methane-, ethane-, propane-, butane-, pentane-, and hexanesulfonate, respectively. (b) A portion of the boxed region in part a, with the abscissa and ordinate expanded.

further changes in the final volumes measured. All measurements were made in triplicate and averaged.

Frequencies at which the absorbance maxima ( $\lambda_{\max}$ ) of difference spectra occur were determined by curve-fitting the positive peaks of each difference spectrum with single-component, mixed Lorentzian and Gaussian functions using an iterative, linear least-squares algorithm ("Fit"; Galactic Industries Corp.).

**Osmolality Measurements.** The osmolality of each 100 mM sample solution was determined, in duplicate, using the method of freezing point depression on an appropriately calibrated Model No. 3D2 advanced digimatic osmometer.

## Results

A typical infrared absorbance spectrum of liquid water is shown in Figure 1 (spectrum 1). In the 3800–2800-cm $^{-1}$  region of the spectrum there is a broad absorption envelope corresponding to a large series of individual overlapping bands that represent transitions separated by small energy differences. The major families of transitions<sup>15</sup> originate in a high-frequency asymmetric stretch,  $\nu_3$  ( $\leftarrow$ H-O $\rightarrow$ -H), and a lower frequency symmetrical stretch,  $\nu_1$  (H $\rightarrow$ O $\leftarrow$ H).<sup>16</sup> Previous work has established that both  $\nu_3$  and  $\nu_1$  shift to lower frequencies as water–water hydrogen bonds are formed.<sup>17</sup> The precise energy of these transitions is a complex function of the number, length, and geometry of the intermolecular hydrogen bonds.<sup>17</sup>

(15) Herzberg, G. *Infrared and Raman Spectra of Polyatomic Molecules*; D. Van Nostrand Company: Princeton, NJ, 1945.

(16) Water's three normal modes of vibration are presented schematically: [ $\nu_1$  H $\rightarrow$ O $\leftarrow$ H], [ $\nu_2$   $\leftarrow$ H-O-H $\rightarrow$ ], [ $\nu_3$   $\leftarrow$ H-O $\rightarrow$ -H] ( $\nu_2$  occurs in the 1600-cm $^{-1}$  region of the spectrum and will not be discussed in this report.)

(17) (a) Pimentel, G. C.; McClellan, A. L. *The Hydrogen Bond*; W. H. Freeman and Company: San Francisco, CA, 1960. (b) Glew, D. N.; Rath, N. S. *Can. J. Chem.* 1971, 49, 837. (c) Lindgren, J.; Tegenfeldt, J. *J. Mol. Struct.* 1974, 20, 335.

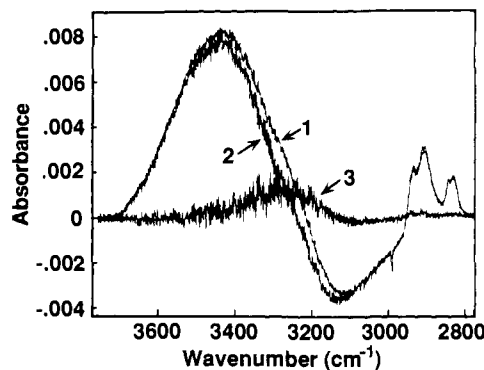


**Figure 3.** Solutions of hexanesulfonate (100 mM) were measured in a GeAsSe cell (spectrum 2) as well as in a ZnSe cell (spectrum 1). Spectrum 3 is the difference spectrum that results from subtracting spectrum 2 from spectrum 1 and demonstrates that no significant differences exist between the spectra obtained in the different cells.

Figure 1 shows the difference (spectrum 2) that results from subtracting two independently measured water samples, demonstrating the reproducibility of the measurement process. Spectrum 3 is the difference spectrum of an aqueous solution of 100 mM sodium hexanesulfonate, illustrating how small the differences are between a spectrum of pure water and that of a representative experimental solution.

Aqueous solutions of a series of model compounds, consisting of hydrocarbon chains of varying length (linked to a sulfonate group to provide water solubility), were examined. Individual difference spectra are shown in Figure 2. Each difference spectrum has the same general features: a high-frequency positive component (centered at  $\sim 3400\text{--}3500\text{ cm}^{-1}$ ) and a low-frequency negative component (centered at  $\sim 3125\text{ cm}^{-1}$ ). (Absorption bands in the  $2800\text{--}3000\text{ cm}^{-1}$  region reflect hydrocarbon vibrations.)

An important pattern is apparent when the alkanesulfonate difference spectra are compared. With increasing hydrocarbon length, both the positive and negative components of the difference spectra become increasingly larger in absolute value (Figure 2). One exception occurs with the methanesulfonate difference spectrum: the negative component is intermediate in value between the pentane- and hexanesulfonate difference spectra.

The difference spectra associated with the alkanesulfonate solutions are clearly different from the difference spectrum associated with a simple aqueous solution of sodium sulfate (Figure 2a, spectrum 2), which is a reasonable control for the sodium sulfonate moiety.

Comparing the difference spectra of the sulfonate compounds reveals a progressive shift (to lower energy) in the frequency at which the positive peaks have their maximum absorbance values ( $\lambda_{\text{max}}$ ): methanesulfonate,  $3466\text{ cm}^{-1}$ ; ethanesulfonate,  $3450\text{ cm}^{-1}$ ; propanesulfonate,  $3448\text{ cm}^{-1}$ ; butanesulfonate,  $3445\text{ cm}^{-1}$ ; pentane- and hexanesulfonate,  $3440\text{ cm}^{-1}$ .

The negative component of each alkanesulfonate spectrum is significantly asymmetrical (Figure 2a). For this reason the relatively simple methods used to identify the positions of the positive peak maxima were not applicable, and more sophisticated methods of quantitative analysis are now being applied. Visual inspection of the negative peaks does not reveal any significant differences in the frequencies at which peak minima occur.

To prove that the spectra described above did not result from artifactual interactions between either solvent or solute molecules and the crystalline surfaces of the internal reflectance cells used in the measurement process, samples of neat water and hexanesulfonate were measured in a GeAsSe cell as well as in the ZnSe cell used for all other samples (100 mM sample concentration,  $\text{pH } 7.0 \pm 0.1$  and  $24.0 \pm 0.1\text{ }^\circ\text{C}$ ). No significant differences were found between spectra obtained in the different cells (Figure 3).

To prove that the alkanesulfonates do not absorb in the  $3000\text{--}3800\text{ cm}^{-1}$  region where water vibrations occur, 100 mM hexanesulfonate was measured in both  $\text{H}_2\text{O}$  and  $\text{D}_2\text{O}$  ( $\text{D}_2\text{O}$  itself has no absorptions in this region). In  $\text{D}_2\text{O}$  the hexanesulfonate

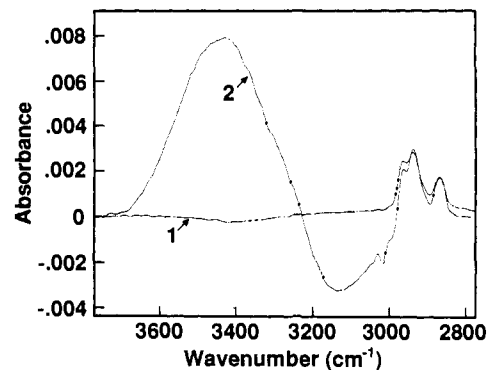


**Figure 4.** Hexanesulfonate (100 mM) was measured in  $\text{H}_2\text{O}$  (spectrum 2) and  $\text{D}_2\text{O}$  (spectrum 1) at  $\text{pH(D)} 7.0 \pm 0.1$  (the pD of the  $\text{D}_2\text{O}$  solution was measured on a pH meter without correcting for any isotopic effects).  $\text{D}_2\text{O}$  itself has no absorptions in this region. In  $\text{D}_2\text{O}$ , the hexanesulfonate shows no significant absorption in the relevant region.

shows no significant absorption in the relevant region (Figure 4).

To ensure that the alkanesulfonates were examined under monomeric conditions, the osmolality of each sample solution was measured (in duplicate). Ideal monomeric 100 mM solutions of the sodium alkanesulfonates would have osmolalities of 0.2000 osm/kg. The averaged measured values were as follows (all units = osm/kg): methanesulfonate, 0.1920; ethanesulfonate, 0.1905; propanesulfonate, 0.1945; butanesulfonate, 0.1870; pentanesulfonate, 0.1995; hexanesulfonate, 0.1975. The largest variation between duplicate measurements for any sample was 0.007 osm/kg. These measurements indicate that the solutes were examined as monomers. This result is not surprising since the critical micelle concentration of hexanesulfonate is 0.5 M and that of pentanesulfonate is  $\sim 1.0\text{ M}$ .<sup>18</sup>

## Discussion

The spectra of water in the presence of various sodium alkanesulfonates differ from the spectrum of pure water. Shifts in absorbance intensities and frequencies reflect changes in populations of water molecules with different hydrogen-bonding patterns.<sup>17</sup>

The negative peak in each sodium alkanesulfonate difference spectrum (e.g., Figure 2a) reflects loss of water molecules from "pure bulk" solvent as water is partitioned into newly formed hydration shells. It is possible that the observed negative peaks may not represent all of the water populations that are depopulated when a solute is dissolved. Higher energy negative peaks may be present but not observed because they are obscured by positive bands that occur in the same region of the spectra. The asymmetry of the observed negative peaks is caused by a proportionally greater loss of water molecules with higher frequency vibrations (i.e., fewer numbers of intermolecular hydrogen bonds<sup>17</sup>), compared to the distribution of states found in bulk solvent in this region of the water vibrational spectrum.

The positive peak in each sodium alkanesulfonate difference spectrum (e.g., Figure 2a) represents water molecules that have partitioned into solvation shells that surround both the ionic moieties (i.e.,  $\text{Na}^+$  and  $-\text{SO}_3^-$ ) and the hydrocarbon moieties present in each solution. It is interesting to note that the positive peaks associated with hydration-shell water molecules are found at higher frequencies than the negative peaks that represent the depopulation of bulk water. This implies that the hydration shells contain fewer average hydrogen bonds per water molecule than the bulk solvent.<sup>17</sup> Similar shifts to frequencies higher than that of bulk water have been observed previously for solutions containing inorganic solutes.<sup>12e</sup> We also have observed high-energy frequency shifts in the difference spectra associated with inorganic salt solutions, including  $\text{Na}_2\text{SO}_4$  (Figure 2) as well as  $\text{NaCl}$ ,  $\text{NaBr}$ ,

(18) (a) Lelong, A.; Tartar, H.; Lingafelter, E.; O'Loane, J.; Cadle, R. *J. Am. Chem. Soc.* **1951**, *73*, 5411. (b) Mukerjee, P.; Mysels, K. *Critical Micelle Concentrations of Aqueous Surfactant Systems*; U.S. Government Printing Office: Washington, DC, 1971.

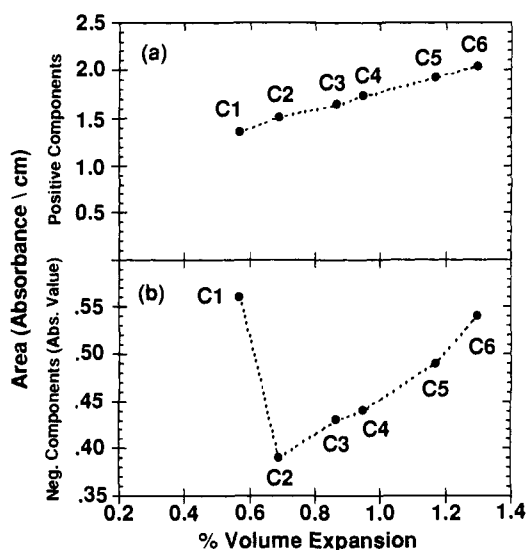


**Figure 5.** (a) The areas beneath the positive peaks of the alkanesulfonate difference spectra (Figure 2) plotted against the liquid volume expansions that occur when the relevant solutes are dissolved in water to form 100 mM sample solutions. The points labeled C1–C6 represent sodium methane-, ethane-, propane-, butane-, pentane- and hexanesulfonate solutions, respectively. (b) The absolute values of the areas beneath the negative peaks of the alkanesulfonate difference spectra plotted against the volume expansions that accompany solute dissolution (as described for part a).

NaI, KCl, KBr, KI (data not shown, manuscript in preparation).

Since the same ionic moieties are present in each of the sodium alkanesulfonate solutions and since all solutions were measured under the same experimental conditions (including concentration, pH, and temperature), any differences in the intensities or frequencies in the difference spectra of the alkanesulfonate solutions can be attributed to differences in the hydrocarbon moieties. For instance, the values of  $\lambda_{\max}$  for the positive peaks in the ethane- to hexanesulfonate (C2–C6) difference spectra demonstrate a progressive shift to lower energy (3450–3440  $\text{cm}^{-1}$ ) as the hydrocarbon length is increased. This shift is consistent with an increase in the numbers of intermolecular hydrogen bonds present in the hydration shells.<sup>17</sup>

The observed difference spectra may result from two phenomena. The water molecules that form the hydration shells experience an overall shift to higher vibrational frequencies when an alkanesulfonate is dissolved. This may be largely due to the ionic portions of the solutes. The shift to higher frequency is moderated by the amount of hydrocarbon present on the solute and results in the reported direct correlation between hydrocarbon length and decreasing values of  $\lambda_{\max}$ .

The absolute value of the area beneath each negative and positive peak in the C2–C6 series of difference spectra correlates with the experimentally measured size of the relevant solute in aqueous solution (Figure 5). This means that the negative and positive peak areas reflect the numbers of water molecules that are lost from bulk solvent and that are present in the hydration shells, respectively. This also means that the hydration shells associated with all members of the C2–C6 series appear to have essentially similar average values for the extinction coefficient ( $\epsilon$ ) of water. However, for any individual member of the C2–C6 series (e.g., propanesulfonate), the negative and positive peak areas are *not* equal. This implies that there are significant differences in the average  $\epsilon$  values associated with pure water and hydro-

carbon-induced hydration-shell water, presumably reflecting altered average covalent bond lengths, bond angles, force constants, and other consequences of the different hydrogen-bonding networks.

Thus, based upon these data, it appears that when a sodium alkanesulfonate is dissolved in water, "pure" water molecules are lost from bulk solvent and form structurally distinct hydration shells around the solute. The number of waters that partition into the solvation shell is directly proportional to the size of the hydrocarbon. The vibrations of these water molecules occur at frequencies that are higher than those of bulk water molecules.

Methanesulfonate is anomalous compared to the larger members of the alkanesulfonate series, in that the absolute value of the area beneath the negative peak of the difference spectrum is larger than the expected value (based upon the C2–C6 results) and does not correlate with the solute size (Figure 5b). The reason for this exception cannot be explained at this time, but may reflect the fact that the methanesulfonate molecule contains only a single methyl group immediately adjacent to a highly ionic sulfonate moiety. Interfacial boundaries between hydrophobic and ionic molecular components may result in hydration shells with structures that are qualitatively different from those induced by either predominantly hydrophobic or ionic species. The absence of CH vibrations (2800–3000  $\text{cm}^{-1}$ ) may also contribute to the anomalous values of the methanesulfonate spectrum. The reasons for the absence of these expected hydrocarbon vibrations are now being examined.

This report introduces an experimental approach that allows hydrophobicity to be evaluated in terms of the structures of bulk water and solute-induced hydration shells. Using this approach, it is possible to quantify changes in the vibrational spectra of hydration-shell water molecules as the methylene and/or methyl content of a solute is increased, i.e., as the "hydrophobicity" of the solute is increased (independent of the increased numbers of waters in the hydration shell). This is seen in the shift of the positive peaks to lower frequencies (Figure 2) and can be interpreted as indicating an increase in the average number of hydrogen bonds per water molecule present in the hydration shell.<sup>17</sup>

With further development of the methods described in this paper, it will be possible to examine enthalpic contributions to solvent hydrogen bond formation, directly probe the interactions between clusters of hydrophobic molecules, evaluate the effects of temperature and pressure on hydrophobic effects, and examine the role(s) of water in stabilizing secondary and tertiary structure in proteins. The information thus gained will lead to a better understanding of the dissolution process and help form the basis for a comprehensive theory of hydrophobic effects.

**Acknowledgment.** We thank our colleagues Jeffrey Skolnick, Darryl Rideout, and Cris Lewis for stimulating discussions. We also thank Martin Karplus and Peter Privalov for reviewing the manuscript and providing valuable suggestions for future experiments. We acknowledge the expertise and talented craftsmanship of Chris Fish and Ward Coppersmith of the Instrumentation and Design Laboratory at The Scripps Research Institute. Lastly, we extend our special appreciation to Richard Lerner, William Beers, and Peter Wright for their support in establishing a vibrational spectroscopy facility at The Scripps Research Institute.

**Registry No.** Methanesulfonic acid, sodium salt, 2386-57-4; ethanesulfonic acid, sodium salt, 5324-47-0; propanesulfonic acid, sodium salt, 14533-63-2; butanesulfonic acid, sodium salt, 2386-54-1; pentanesulfonic acid, sodium salt, 22767-49-3; hexanesulfonic acid, sodium salt, 2832-45-3.